CHAPTER 2

Literature Reviews

The chapter discusses the factors influencing potential of slag formation and deposition in pulverized coal fired boiler, as well as the relevance of the combustion characteristic and the detail about pulverized coal combustion, which affect slagging. Throughout, approaches to solve the slag problem in previous researches were considered.

2.1 Coal Combustion Characteristic

Combustion is the process to convert chemical energy in the fuel to heat. A power plant transforms this heat into power. From the hot combustion products through tubes in the boiler shell and heat transfer to water, water is transformed to steam for driving the steam turbine and generating electricity. To design a power plant, study of combustion characteristic is absolutely necessary.

The coal combustion sequences are shown in Figure 2.1, and the reaction details are as follow (Miller, 2011; Tillman, 1991; Garba, 2012).

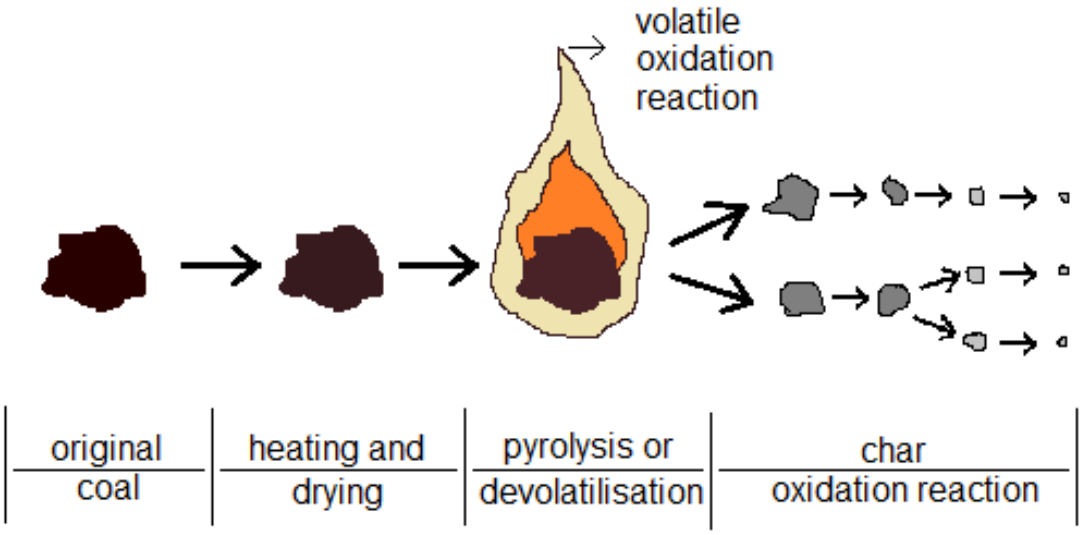

Figure 2.1 The process of coal combustion (Anthony and Preto, 1995)

2.1.1 Heating and drying: the coal particles contain some moisture and are at the ambient temperature. When they enter the furnace, they are heated reactor temperature (about 105°C), moisture is driven off. The process can be represented in Eq. (2.1) (Tillman, 1991). This process is endothermic, which is the precise amount of energy required.

$$Wet\ fuel\ paticle + heat \rightarrow dry\ fuel\ particle + H_2O \quad (2.1)$$

The process involves the evaporation of the surface moisture and the loss of the inherent moisture. The general conduction equation of heat transfer is presented by Eq. (2.2) (Tillman, 1991;Garba, 2012).

$$q = k_c A_p\left[(T_1 - T_2)/r_p\right] \quad (2.2)$$

where q is the the flow of heat, k_c is the thermal conductivity of the coal, A_p is the surface area of the coal particle, T_1 is the temperature at the surface of the coal particle, T_2 is the temperature at the center of the coal particle, and r_p is the radius of the coal particle.

The particle is heated to the pyrolysis reaction temperature in order to give off volatiles, and described by Eq. (2.3) (Williams et al., 2001).

$$C_{p.p}(dT_p/dt) = Q_c + Q_r + Q_v \quad (2.3)$$

where $C_{p.p}$ is the specific heat of the coal particle, T_p is the temperature of the coal particle, Q_c is the coal particle convection of heat transfer, Q_r is the coal particle radiation of heat transfer, Q_v is the coal particle vaporization of heat transfer.

2.2.2 Pyrolysis or devolatilisation: The process is largely endothermic. The step is the heating of the fuel compounds in the absence of oxygen to avoid

oxidation of the carbon, hydrogen, and sulfur. The pyrolysis initiation temperature is around 450-500°C (Garba, 2012). The rate of solid particle pyrolysis may be determined using two types of model for evaluating.

1) Kinetic model

First order kinetics model for solid fuels pyrolysis is proposed by Arrehenius equation as Eq. (2.4) (Tillman, 1991;Garba, 2012; Pintana et al, 2013).

$$k = K_o \exp(-E/RT) \quad (2.4)$$

where k is the rate coefficient, K_o is pre-exponential factor, E is the activation energy, R is the universal gas constant, and T is the absolute temperature.

2) Heat transfer models

Energy is used to transfer into the coal particle, and mass is driven out in the form of volatile products. Energy is transferred to the boundary layer by radiation and convection from the furnace surroundings and though the boundary layer and the particle to the reaction front by conductive heat transfer. The rate of pyrolysis at the reaction zone of the particle is defined by Eq. (2.5).

$$k_t = 1/[C(T)dT + H_v] \quad (2.5)$$

where k_t is the rate constant, $C(T)$ is the heat capacity of the coal particle.

It generates non-condensible light gases, tar and residual char. The relative yields of gaseous species depend on the type of coal and the pyrolysis conditions. The volatiles diffuse into the surrounding, mix

with oxygen in air, and flame is formed. Volatile oxidation reactions occur extremely rapidly.

2.2.3 Char oxidation: The reaction starts when volatile release is largely completed, and oxygen from environment is reached the surface of the char particle. The reaction between the char and oxygen is a gas-solid heterogeneous reaction. The gaseous oxygen diffuses to and into the char particle, being absorbed, and reacted on the pore surface of the particle. The rate of this step varies with coal type, temperature, pressure, char characteristics, and oxidizer concentration (Tillman, 1991).

Garba (2012) described the types of flames in combustion system. There are three different homogeneous flame types with non-premixed, premixed and partially premixed types. In the non-premixed or diffusion flames, a fuel and oxidizer are introduced to the combustion zone in separate streams due to diffusion and mixing before combustion. The non-premixed combustion modelling includes the transport equations, the species concentration, and the turbulent diffusion flames with fast chemistry (Turns, 2006). In contrast to the non-premixed flames, the premixed combustion means the fuel and oxidizer are mixed prior to combustion. The premixed combustion modelling is valid for laminar and turbulent flows with predicts reacting discrete phase particles in the FLUENT package. The partially premixed type is the flame of fuel and oxidizer mixture with non-uniform mixing. The model of partially premixed flame is considered as the combination of non-premixed and premised models.

2.2 Pulverized Coal Combustion in Boilers

The pulverized coal technology is the most widely used in power generation worldwide. The technology is the choice for large industrial boilers and coal-fired electric utility generators (Miller, 2011), because coal can be reduced to powder and burned like gas. Therefore, fires are easily lighted and controlled (Singer, 1981). The main coal size is 65-79% by weight less than 200 mesh (74 μm) for lignites and subbituminous coals and

80-85% less than 200 mesh for bituminous coals, with less than 2% greater than 50 mesh (300 μm) (Berkowitz, 1979). The compositions of coal show large differences, Figure 2.2. Certain portions of coal may be enriched with specific minerals, so after pulverized, the composition of any given particle depends on the local composition of the lump.

After the coals are pulverized, they are transported to the burners by pneumatic conveyor and mixed with primary air. Basically, the pulverized coal firing has coal-air mixture burning in a central nozzle with secondary air coming in around the nozzle as shown in Figure 2.3. First, the volatile matter burns and heats the remaining carbon to incandescence. Then, the secondary air supplies the oxygen to complete the combustion of carbon particles (Kohan, 1997). The flame temperatures in furnace are around 1510°C and the temperature of flue gas exiting the furnace is 1010°C. Heat is lost by radiation in the furnace to waterwalls and superheater/reheater tubes. Some of the remaining heat is extracted to the cool feedwater then the combustion gases through the economizer and to the feed air within the air preheater (Miller, 2011; Edge et al., 2012).

Tangential firing is one of pulverized coal-fired boiler type. Specially, the burners in the furnace, can be tilted upward or downward, thereby changing the temperature of flue gas (Kohan, 1997; Miller, 2011). The ignition at each burner is supported by the flame from the proceeding burner. The pattern of flame imparts a rotating or spinning motion to the flame body (Shields, 1961). The tangential firing provides extremely rapid turbulent combustion with the short length to create a fire ball swirling at the center of furnace. Figure 2.4 shows the example of fire ball from 4 corner burners in the tangentially fired pulverized-coal boiler.

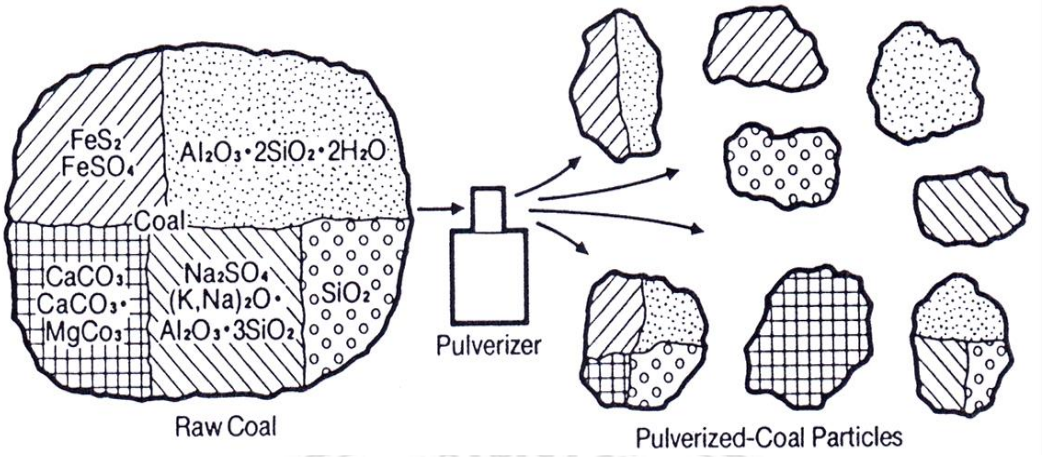

Figure 2.2 Segregation of mineral matter during pulverization (Singer, 1981)

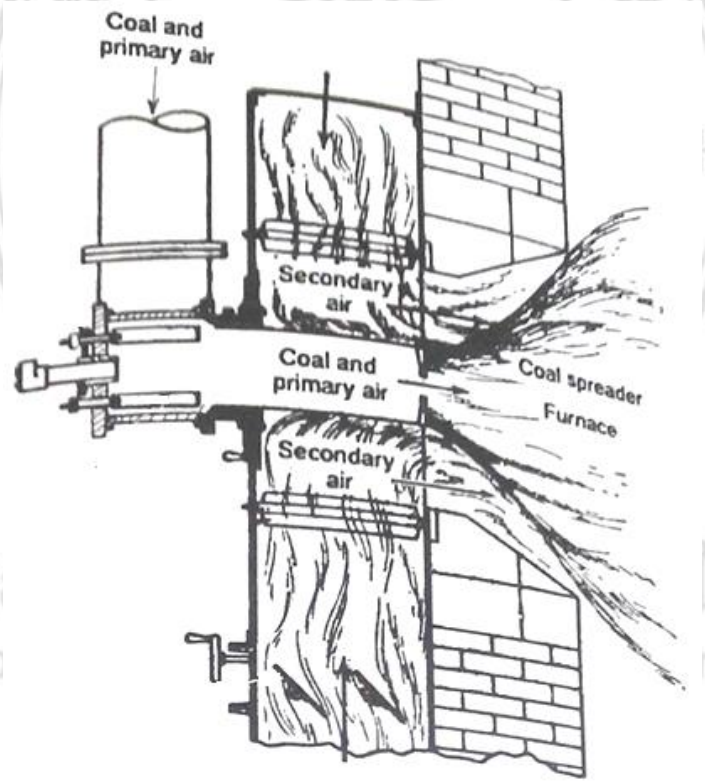

Figure 2.3 The coal-air mixture burning in pulverized coal boiler (Kohan, 1997)

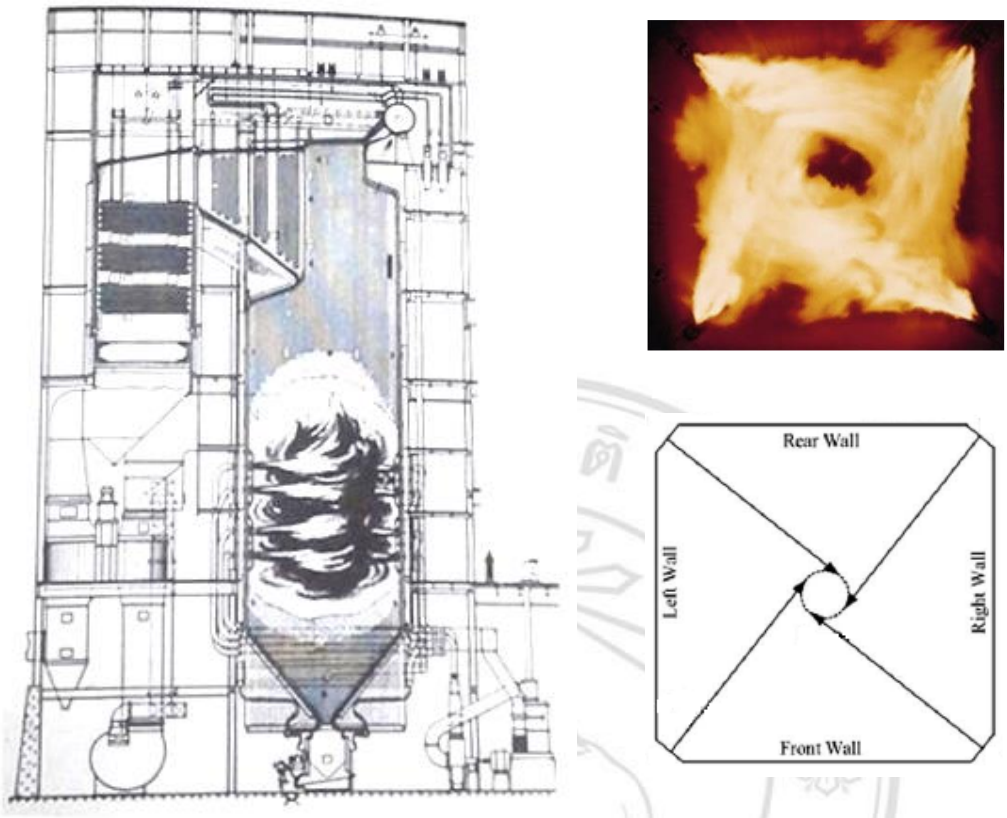

Figure 2.4 The fire ball in tangential fired boiler (Kohan, 1997; Choi and Kim, 2009)

Larsen (2012) gave an overview of mathematical models particular to particle flow and combustion in the complicated interactive processes of pulverized coal combustion by the application of the ANSYS Fluent commercial code based on finite volume method. The ANSYS Fluent is a commercial Computational Fluid Dynamics (CFD) package, that uses the numerical solution with Navier-Stokes equations. Wang and Yan (2008) concluded the basic governing equations in CFD models of the thermochemical processes including fluid flows, heat and mass transfer, and chemical reactions. The following equations are the conservation laws of mass, momentum, energy and species, (Eq. 2.6-2.9), respectively.

$$\frac{\partial \rho}{\partial t} + \nabla \cdot (\rho \vec{u}) = S_p \tag{2.6}$$

$$\frac{\partial (\rho \vec{u})}{\partial t} + \nabla \cdot (\rho \vec{u} \vec{u}) = -\nabla p + \nabla \cdot (\mu \nabla \vec{u}) + S_u \tag{2.7}$$

$$\frac{\partial(\rho H)}{\partial t} + \nabla \cdot (\rho \vec{u} H) = \nabla \cdot (\lambda \nabla T) + S_H \quad (2.8)$$

$$\frac{\partial(\rho Y_i)}{\partial t} + \nabla \cdot (\rho \vec{u} Y_i) = \nabla \cdot \left(D \nabla (\rho Y_i)\right) + S_Y + R_f \quad (2.9)$$

In the program version 13.0, the combustion models are based on these foundations: inert heating, evaporation, devolatilisation, volatile combustion, and char combustion. The steps of simulation are first to set up a case, then run the calculation until convergence, and finally interpret the results. As well as the works from Yin et al. (2012) and Gurba (2012), the steps of the pulverized fired combustion processes numerical simulation have to be followed. Firstly, the computational grid is generated to represent the combustion furnace for the calculations. Then, the available and suitable models in the ANSYS Fluent software, shown in Table 2.1, are set up. The results of the prediction are analyzed and discussed by the post-processing.

Table 2.1 Summarized of the model in combustion simulation (Garba, 2012)

Activity	Model used
Turbulence	RNG k-ε (Standard)
Absorption coefficient	Weighted-Sum-of-Gray-Gases model (WSGGM)
Radiation	Discrete ordinates (DO)
Combustion	Species transport
Particle diameter distribution	Rosin-Rammler
Particle dispersion	Stochastic DRW
Devolatilization	Single rate
Char burnout	Kinetics/diffusion-limited

ANSYS Inc. (2010) and Fluent® (2014) gave the detail of models. The RNG k-ε turbulence model is derived from the Navier-Stokes equations and additional terms and functions in the transport equations for k and ε. The effect of swirl on turbulence is included, to account for swirling flows. These make the results more accurate and reliable for a wider class of flows. The WSGGM is a compromise between the oversimplified gray gas model and a complete model which takes into account

particular absorption bands. The assumption is based on the total emissivity over the distance. However, the model cannot be used to specify the absorption coefficient in each band when using the non-gray DO model or the non-gray P-1 model. The DO radiation model is chosen to solve the radiative transfer equation for a finite number of discrete solid angles, each associated with a vector direction fixed in the global Cartesian system. The species transport model is chosen to solve conservation equations for chemical species, and to predict the local mass fraction of each species through the solution of a convection-diffusion equation. The Rosin-Rammler distribution function is used to define the size distribution of particles by inputting a diameter for the first and last point and using the linear equation to vary the diameter of each particle stream in the group. The stochastic method with the discrete random walk (DRW) model is used to determine the instantaneous gas velocity. The model gave results in strongly nonhomogeneous diffusion dominated flows, where small particles should become uniformly distributed. The single kinetic rate model is chosen such that the rate of devolatilization is first-order dependent on the amount of volatiles remaining in the particle. And the last in the kinetics/diffusion-limited model, the kinetic rate takes the effect of chemical reactions on the internal surface of the char particle as well as the effect of pore diffusion into account. It can be seen that ANSYS Fluent program is suitable for use is simulation of the pulverized coal combustion boiler.

Black et al. (2013) gave the detail of heat transfer to the walls and tube walls model. The 330 W/m^{2}K of overall resistivity was used, which incorporated the resistivity due to the deposition layer, metal tube wall and steam side film heat transfer coefficient (Edeg et al., 2012). It can be calculated by Eq. 2.10.

$$\dot{q} = u_o(T_{w,o} - T_s) \tag{2.10}$$

where $\dot{q}$ is heat flux (W/m^2), u_o is partial overall admittance factor (W/m^{2}K), $T_{w,o}$ is outer wall temperature (K), and T_s is steam phase wall temperature (K)

Tian et al. (2009) applied the commercial CFD (ANSYS/CFX 12.0) for predicting the pulverized brown coal combustion process of a 375 MW tangentially-fired furnace in

Australia. The 2 steps of reaction in Eqs. 2.11-2.14 were used to model the coal combustion process, similar to Black et al. (2013). The standard k-ε and SST model were compared. The results gave similar predictions and good agreement with the measured plant data.

$$Coal \rightarrow Volatiles + O_2 \tag{2.11}$$

$$Volatiles(HC) + O_2 \rightarrow CO + H_2O \tag{2.12}$$

$$C(Char) + 0.5O_2 \rightarrow CO \tag{2.13}$$

$$CO + 0.5O_2 \rightarrow CO_2 \tag{2.14}$$

Although the tangential fired boilers are the most widely used type for industrial coal combustion, there are still some problems such as combustible matter in fly ash, combustion instabilities at low loads, and slagging in the furnaces (Fan et al., 2001; Choi and Kim, 2009). The pulverized fired boiler has been found to have large slag deposits, in the Table 2.2. Especially, use of low grade coal is more adverse in reducing the performance of the coal-fired boiler and increasing the environmental impact (Bosoaga et al., 2006).

Most researches focus on developing the combustion technology for high efficiency, studying the influential parameters on the operation and emission control of pulverized coal-fired power plants (Bonin and Queiroz, 1991; Williams et al., 1994; Bonin and Queiroz, 1996; Eastwick et al., 1999; Suda et al., 2002; Yin et al., 2002; Tanetsakunvatana and Kouprianov, 2003; Buhre et al., 2005; Kuprianov and Tanetsakunvatana, 2005; Backreedy et al., 2006; Belosevic et al., 2006; Bris et al., 2007; Asotani et al., 2008; Choi and Kim, 2009; Schaffel et al, 2009; Wall et al., 2009; Tian et al., 2009; Filkoski, 2010; Modlinski, 2010; Al-Abbas et al., 2011; Chen et al., 2012; Khamsimak et al., 2012; Al-Abbas et al., 2013; Agraniotis et al., 2009 b.). Slag problem has also been studied extensively.

Table 2.2 Overview characteristic description and specific location of slag in pulverized coal fired boiler (Zygarlicke et al., 2001)

Boiler zone	Brief description of slag characteristic
Waterwalls, lower, middle radiant boiler regions	Dense, highly sintered or molten slag deposits covering patches or entire waterwall areas, up to several centimeters or 2 inches thick
Rim around burners, called “eyebrows”	Sticky ash rimming or accumulating on the waterwalls near burners
Lower furnace radiant zone	Highly-fused, metallic-looking and often several centimeters or up to 2 inches thick
Waterwalls directly or at 2-3 meters above burners	Highly-fused, very porous slag typically with a bubbly appearance; termed vesicular slag

2.3 Slag Problem in Boiler

Slagging problem can have a negative effect on total plant performance, causing loss of capacity, loss of heat, boiler equipment damage, loss of time and cost in maintenance of the boilers (Laursen et al., 1998; Hare et al., 2010; Pintana et al., 2014 a;).

Benson et.al (1995) gave an overview of research related to coal ash in the boiler, including the problem of the behavior of ash in the advanced technologies that use coal. Focus was on lignite and sub-bituminous in the U.S. It was found that the accumulation of ash in pulverized coal combustion was high with high calcium coal.

Erickson et.al (1995) studied fouling and slagging in boilers using coal as fuel. They began with the deposition of small particles, and subsequent melting of the particles and the final layer is a fluid. Sub-model validation for slag deposition growth and heat transfer was carried out using data from well-controlled, pilot-scale combustor testing. Composition of the different layers within the deposit was compared with the model

prediction to validate the ash particle stickiness model. In addition, the measured temporal heat flux profile was used to check the consistency of the parameters describing the deposit growth sub-model.

Hare et al. (2010) reviewed slagging as mainly a molten deposit of ash particles which contacts the boiler tube surface. Soot blowers can be used to clean the slag during operation. But, this method can only remove slag on the tubes at very low rate.

Pintana and Tippayawong (2014) studied slag formation and deposition on pulverized coal boilers at Mae Moh power plant. The soot blowers may not be able to handle when slag in the boiler furnace becomes excessive. In related works by Pipatmanomai et al. (2009) and Luxsanayotin et al. (2010), the cause of occasional slagging problems in Mae Moh power plant was examined.

2.3.1 Characterisation of Slag

Several reviews relating to the slag characteristics have already been reported.

Jak (2002) investigated the microstructure of coal ash slag after reaching the AFT temperature test by the scanning electron microscopy (SEM) and the energy dispersive spectra analyzer (EDS). The electron probe X-ray microanalyzer (EPMA) and wavelength dispersive detectors (WDD) were used to measure phase compositions.

Lopez et.al (2004) studied properties of the ash slagging by various methods, including.

1) Mechanical properties: Total deposition rate (TDR), porosity, strength, viscosity, fusion behavior (use of a Thermo-Mechanical Analyser, TMA), and ash particle size.

2) Thermal properties: Conductivity (through the tube together with the deposit) and radiative properties.

3) Chemical properties: Chemical composition of coal (by thermogravimetric, TGA) in terms of proximate analysis and ultimate analysis. Ash compositions are commonly determined by several different analytical method, e.g. inductively coupled plasma (ICP) with optical emission spectroscopy (OES) or with mass spectroscopy (MS), X-ray fluorescence (XRF), ion chromatography (IC), atomic absorption spectroscopy (AAS). The method for characterization of deposit samples is the scanning electron microscope (SEM) with EDS analysis, specially when combined with computational calculations (CCSEM-EDX). Finally, quantitative X-ray Diffraction (XRD) can be applied to both ash and deposits for the determination of mineral phases.

Fernandez-Turiel et.al (2004) studied mineral structure and chemical properties of high calcium ash of Agios Dimitrios lignite coal in Greece. It was observed that all surfaces of the boiler were covered with a layer of particles. Analyses using SEM, EDS, XRD, ICP-MS and ICP-OES showed the status indicator of calcium in ash melting of anhydrite ($CaSO_4$), calcite ($CaCO_3$), portlandite ($Ca(OH)_2$) and lime (CaO). In addition, the silicon content of bottom ash and fly ash in the presence of the mineral was quartz (SiO_2), gehlenite ($Ca_2Al_2SiO_7$), and anorthite ($CaAl_2Si_2O_8$).

Papastergios et al. (2005) extended the research of Fernandez-Turiel et.al (2004). The slag deposits were investigated on the chemical composition and behavior by ICP-OES and ICP-MS. The results showed that the most abundant was calcium in the all samples. The conclusion of this research was that the chemical composition of the feed lignite and the co-excavated sterile materials influenced the composition of ash and slag.

Van Dyk et.al (2009) suggested that the composition and structure of minerals in the coal was essential for deformation and accumulation of ash in combustion furnace. In this work, coal from South Africa has been analyzed as follows.

1) Proximate analysis (SABS 924, ISO 1171 and ISO 562)
2) Ultimate analysis (ASTM D4239 and ASTM D5373)
3) Ash flow temperature under oxidizing conditions to 1600°C (ASTM D1857)
4) Ash constituent analysis (ASTM D3682)
5) Calorific value (ISO 1928)
6) Maceral analysis and rank (ISO Standard 7404-2, 1985, ISO Standard 7404-3, 1994)
7) Morphological and chemical analysis (Scanning electron microscopy point count, SEMPC and Computer-controlled scanning electron microscopy, CCSEM)

In summary, the main elements in coal were composed of kaolinite, quartz, aluminosilicates, pyrite, dolomite, calcite. Calcium, in form of dolomite and calcite, was observed from Figure 2.5.

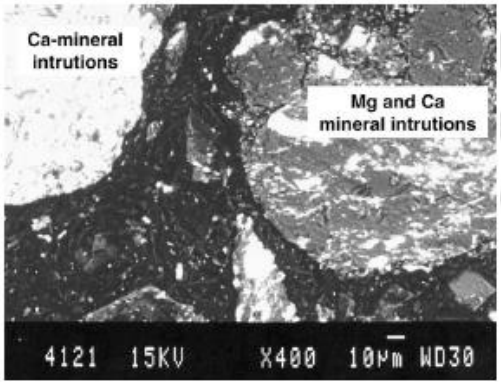

Figure 2.5 Morphological and composition of the ash obtained from SEM (Van Dyk et.al, 2009)

Song et al. (2010) analyzed the chemical composition, the mineral complexes, and the microstructure of Chinese coal slag by XRF, XRD, and SEM, respectively. The Shimaszu XRF-1800 with Rh target X-ray tube, that operated at 50kV and 40mA was used. The results showed enriched glass form of oxide (SiO_2+Al_2O_3 more than 70%). The Rigubu D/max 2550 x-ray powder diffractometer operated with Cu Kα radiation, 40kV, 450mA, step size 0.01° between 2θ = 10° and 80°. The results showed slag that was mainly of amorphous/vitreous character. The JSM-6360LV SEM was used to operate at 5kV. Figure 2.6 showed only spherical particles and no agglomerated particles.

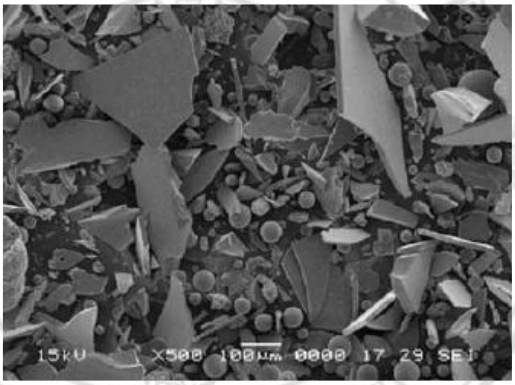

Figure 2.6 SEM micrograph of slag (Song et al., 2010)

Li et al. (2011) studied slag formation mechanism of the process using fluid-bed gasification, mixed samples of graphite and 450 °C Xiaolontan (XLT) ashes treated with different temperatures. The samples and the block slag formed during the testes of XLT were examined by SEM-EDX and XRD (Liu et al., 2013). The results showed that most elements in the iron and silicon slag mechanism before the slag was a partially vitreous materials, and were characterized by fused calcium. The reaction involved may be as follows.

$$pyrite(FeS_2) \rightarrow pyrrhotite(FeS) + other\ sulfides \quad (2.15)$$

$$anhydrite(CaSO_4) \rightarrow calcium\ oxide(CaO) + sulfur\ dioxide(SO_2) \quad (2.16)$$

$$anhydrite\ (CaSO_4) + hydrogen(H_2) \rightarrow oldhamite(SO_2) \quad (2.17)$$

$$magnesium\ \ ferrous\ oxide\ ((MgO)_{0.77}(FeO)_{0.23}) + silicon\ \ dioxide\ (SiO_2)$$
$$\rightarrow\ ferrousmagnesium\ silicate\ (Fe_{0.24}Mg_{0.76}SiO_3) \quad (2.18)$$

$$metakaolin(Al_2O_3 \cdot 2SiO_2) \xrightarrow{900^\circ C} mullite\ (3Al_2O_3 \cdot 2SiO_2) \quad (2.19)$$

$$mullite\ (3Al_2O_3 \cdot 2SiO_2) + calcium\ oxide(CaO) \xrightarrow{950^\circ C}$$
$$anorthite(CaO \cdot Al_2O_2 \cdot 2SiO_2) \quad (2.20)$$

$$anorthite(CaO \cdot Al_2O_3 \cdot 2SiO_2) + calcium\ oxide(CaO) \rightarrow$$
$$gehlenite(2CaO \cdot Al_2O_3 \cdot SiO_2) \quad (2.21)$$

$$goethite(\alpha - FeO(OH)) \rightarrow wustite\ (FeO) \quad (2.22)$$

$$Illite\ (KAL_2[(OH)_2\ AlSi_3O_{10}]) + wusite\ (FeO) \xrightarrow{900^\circ C}$$
$$almandite\ (3FeO \cdot Al_2O_3 \cdot 3SiO_2) + hercynite\ (FeO \cdot Al_2O_3)$$
$$+leucite\ (KAlSi_2O_3) \quad (2.23)$$

$$mullite\ (3Al2O3 \cdot 2SiO2) + wusite\ (FeO) \rightarrow$$
$$3\ fayalite(2FeO \cdot SiO_2) + hercynite(FeO \cdot Al_2O_3) \quad (2.24)$$

$$fayalite\ (2FeO \cdot SiO_2) + calcium\ \ oxide\ (CaO) + silicon\ \ dioxide\ (SiO_2)$$
$$\rightarrow hedenbergi\ te\ (CaO \cdot FeO \cdot 2SiO_2) \quad (2.25)$$

It can be seen that the past research used interesting tools and methods for analyzing the slag characteristics. Some of the tools and methods will be used to measure and analyze the slag from a boiler furnace of EGAT Mae Moh power plant.

2.3.2 Factors Influencing the Slag Potential

Vasquez and Ma (2004) and Ma et al, (2007) studied slag formation and deposition in tangentially-coal-fired boilers. They reported that the slag deposition depended on fuel composition, boiler design, and operating conditions.

Akiyama (2011) and Frandsen et al. (2009) reported that slag phenomena were influenced by factors such as the type of coal (ash compositions, melting temperature and distribution of mineral matter), reaction atmosphere, particle temperature, surface temperature of heat exchanger tubes, tube materials, and flow dynamics.

Vassilev et.al (1995) studied the influence of mineral and chemical composition of samples 43 samples of coal ash melting behavior. The relationship between the oxide and the melting temperature of the ash were found. The melting temperature was dependent on the coal rank and the proportion of components that acted as an aid to fusion (fluxing). These included sulfate, silicate, and oxides of other elements such as anhydrite, acid plagioclases, K feldspars, Ca silicates, and hematite. The high melting temperature was due to a decrease in the mineral that acts as a fluxing and an increase in the mineral acts as a reducing furnace (refractory minerals) such as quartz, metakaolinite, mullite, and rutile, which resulting from the addition of Si, Al and Ti. It was concluded that when the amount and type of minerals in coal and ash changed during the heating temperature of the refractory minerals and fluxing minerals, it was able to explain and predict the behavior of fusion of ash reliably.

Wee et.al (2005) studied effect of burning conditions on the deformation of minerals and the adhesion of ash in boiler furnaces that use sub-bituminous coal as fuel. The study found that increasing the amount of primary air led to good behavior of the ash during combustion. Ash formation was only loosely, if not increase the primary air. The formation of ash melting furnace wall was formed to create a strong bond with such compounds aluminosilicate with a glassy mass. In addition, the formation of the compound to ferrous iron indicated that the ash sticked to the wall furnace through an environment with less oxygen. Changes of K, Ca, Fe and P in the aluminosilicate had important impact on the ash melting furnace walls that formed a viscous texture.

Singer (1981) reported the parameters that affect coal-ash behavior perform to furnace slagging. Ash fusibility temperatures were measured the performance of slagging buildup. Normally, the temperature gap from initial deformation temperature to fluid temperatures indicated that the wall slag was thin, running and tenacious. The parameters correlated with coal-ash compositions that classified to acidic oxide and basic oxides. The acidic oxide (SiO_2, Al_2O_3, TiO_2) were considered to produce high melting temperatures. While, the high proportion of basic oxides (Fe_2O_3, CaO, MgO, Na_2O, and K_2O) in ash affected to low fusibility temperatures. There were many other parameters related with the ash components,

$$\frac{Basic\ oxides}{Acid\ oxides} = \frac{Fe_2O_3+CaO+MgO+Na_2O+K_2O}{SiO_2+Al_2O_3+TiO_2} \quad (2.26)$$

The main ash compositions affecting the deposition behavior were based on base to acid ratio (B/A). It can be calculated from Eq. (2.26), correlated with Pipatmanomai et al. (2009), Song et al. (2009) a, Agraniotis et al. (2009 a). The base/acid ratio reflected a potential for ash-containing metals to combine in the combustion process to produce low melting salts. Extremes at either end of the base/acid ratio indicated a minimum potential for

forming combinations with low fusibility temperatures. Although the base/acid ratio was an indication of the fusion characteristics and slagging potential of a coal ash, it should not be used as the sole criterion of evaluation. A base-acid ratio in the range of 0.4-0.7 showed low ash fusibility temperatures and a higher slagging potential. Agraniotis et al. (2009 a) reported slagging potential of the B/A ratio, defining that the lower range of the slag was less than 0.2, a value between 0.2-1.0 showed medium deposition tendency, and values greater than 1.0 indicated high potential.

The silica/alumina ratio in Eq. 2.27 was used to decide two coals with equal base/acid ratios. The general range of values was between 0.8 and 4.0. This ratio can provide additional information relating to ash fusibility. As both of these constituents are acidic and, therefore, considered high melting as oxides, silica is more likely to form lower melting species (silicates) with basic constituents than alumina. For two coals having equal base/acid ratios, the one with a higher silica/alumina ratio should have lower fusibility temperatures.

$$\frac{SiO_2}{Al_2O_3} \tag{2.27}$$

The iron/calcium ratio, defined in Eq. (2.28), indicated that the base/acid ratio does not account for differences in fluxing action. Among the five basic-oxide components, iron and calcium are the most important, primarily because they make up the largest amount of the basic constituents. Iron oxides comprise 5 to 40 % of the ash and calcium oxides make up 2 to 30 %. The iron-calcium relationship may be related the fusibility of ash. In the absence of lime (CaO), iron oxides do not make the most fusible slags. Ferric oxide, up to about 20%, has a fluxing effect which increases with the percentage. But, above 20 and up to 40%, it does not materially increase the fusibility. The combined fluxing effect of iron oxides and lime has a complex relation to the percentage of the two fluxes. For ashes in which the

percentage of iron oxide is over 14%, the addition of a given lime produces a lowering of the fusion temperatures greater than the same additional percentage of iron oxide. The quantity of magnesia present in coal ashes is usually smaller than the lime; its fluxing effect with lime present is greater than that of an equal additional amount of lime in about the ratio of 3:2.

$$\frac{Fe_2O_3}{CaO} \tag{2.28}$$

And the last parameter is defined in Eq. (2.29). The iron/dolomite ratio is essentially identical to the Fe_2O_3/CaO ratio. CaO and MgO have been found to have similar fluxing properties, and the use of this ratio is recommended when the MgO content of the ash is high. Bituminous-type ash is characterized by iron-oxide/dolomite ratio greater than one, while lignitic ash has Fe_2O_3/CaO+MgO in ratio less than one.

$$\frac{Fe_2O_3}{CaO+MgO} \tag{2.29}$$

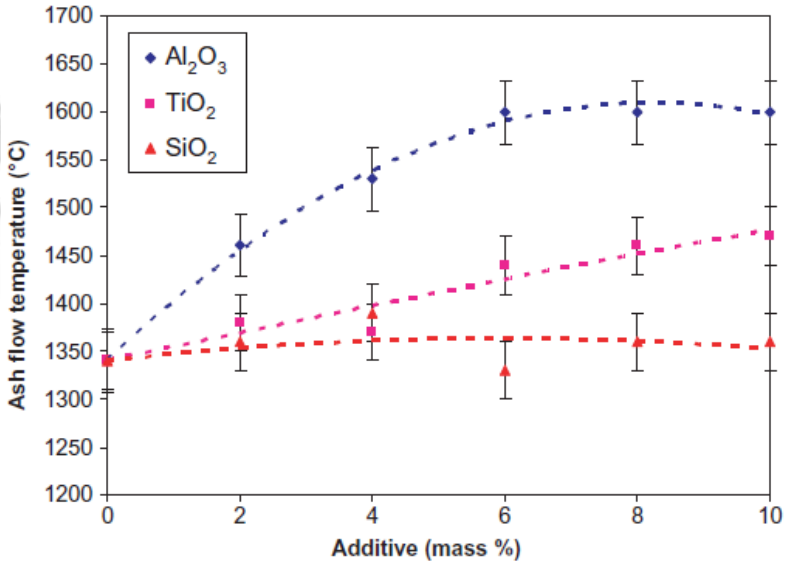

Figure 2.7 Effect of composition of ash (SiO_2, Al_2O_3, and TiO_2) to the AFT (Van dyk, 2006)

Van dyk (2006) studied the influence of the oxides in acids, including Si, Al and Ti on the flow properties of bituminous coal ash. The addition of these oxides was found to increse the ash fusion temperature, shown in Figure 2.7.

Mclennan et.al (2000) studied Iron-Based slagging indicator that was affected by burning coal power in the oxidizing and reducing states. Indication of the slag is shown in Table 2.3. It was found that pyrite was the most important factors, used to explain the slag.

Table 2.3 Summary of slagging indices (Mclennan et.al, 2000)

Index	Ash fusibility	Viscosity	Ash chemistry
Calculation	$\frac{4IDT + HT}{5}$	$\frac{T_{250(ox)} + T_{1000(red)}}{975F_s}$	$\frac{Basic\ oxides}{Acid\ oxides}$
Slagging potential			
low	>1343°C	<0.5	<0.6
medium	1232-1343°C	0.5-0.99	0.6-2.0
high	1149-1232°C	1.0-1.99	2.0-2.6
severe	<1149°C	>2.0	>2.6

where IDT = initial deformation temperature

HT = hemispherical temperature

$T_{250(ox)}$ = 250 poise temp for oxidizing conditions

$T_{1000(red)}$ = 1000 poise temp for reducing conditions

F_s = correlating factor

Basic oxides = Fe_2O_3, CaO, MgO, Na_2O, and K_2O

Acid oxides = SiO_2, Al_2O_3, and TiO_2

S = % sulfur dry coal

Pipatmanomai et al. (2009) studied properties and composition of the lignite coal and ash. The element content was measured for collected fly ashes, bottom ashes and slags, and compared with those of the feed lignite. The

analysis and operational data obtained during the 7-day sampling period were compared with those obtained from the additional laboratory investigation of high Ca lignites (20-57%).

The results showed that the main components were Si, Al, Ca and Fe. Mg, K, P, Ti, Mn and Na were in small amounts, shown in Figure 2.8. The amount of Si and Al oxides were in the form of 43-52% by weight of ash while the oxides of Ca and Fe were 26-32% by weight of ash. Oxide in ash content also affects the melting temperature, shown in Figure 2.9. Increasing CaO resulted in lower melting temperature. Figure 2.10 shows SiO_2 + Al_2O_3 and CaO + Fe_2O_3 increased in the proportion of oxide that was best correlated linearly with the reduction in the proportion of acidic oxides. The power problem of ash melting proportion of oxide wais based on acid.

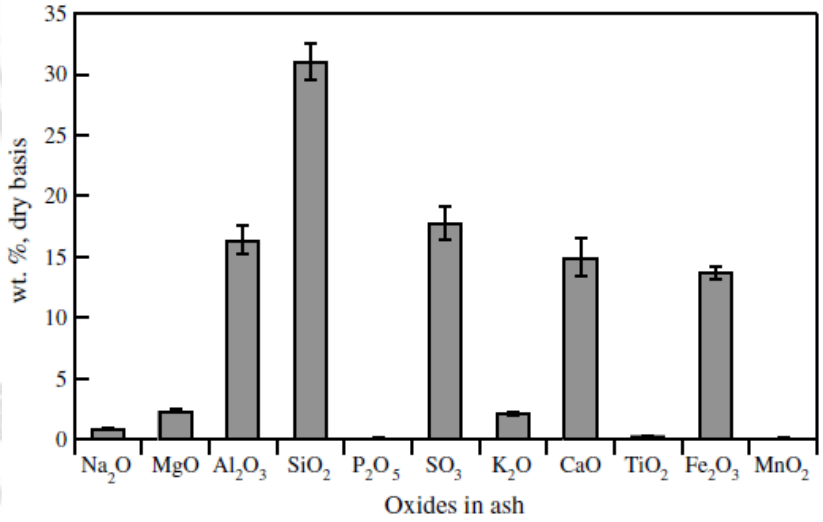

Figure 2.8 Oxide (wt%) in ash prepared from lignite samples collected during the 7-day sampling (Pipatmanomai et.al, 2009)

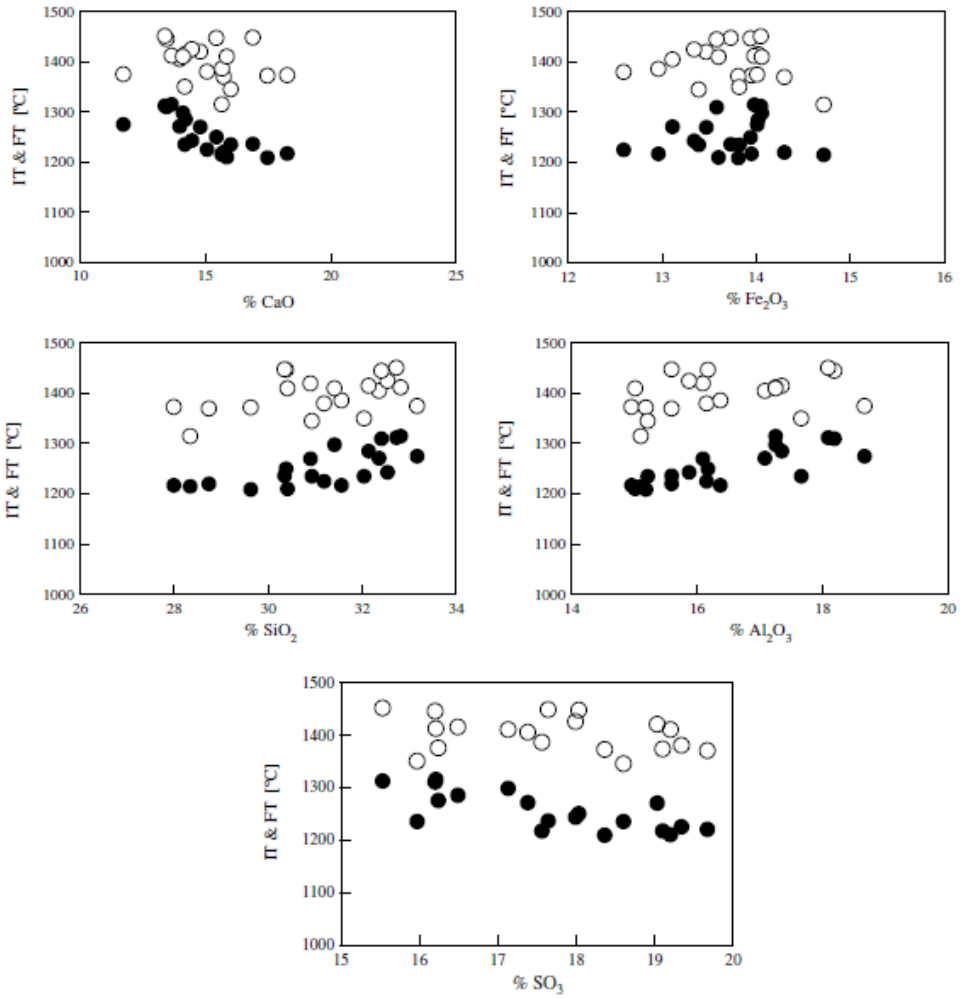

Figure 2.9 Ash fusion temperature as a function of major oxide concentration in laboratory-prepared ashes from lignite during 7-day sampling (Pipatmanomai et.al, 2009)

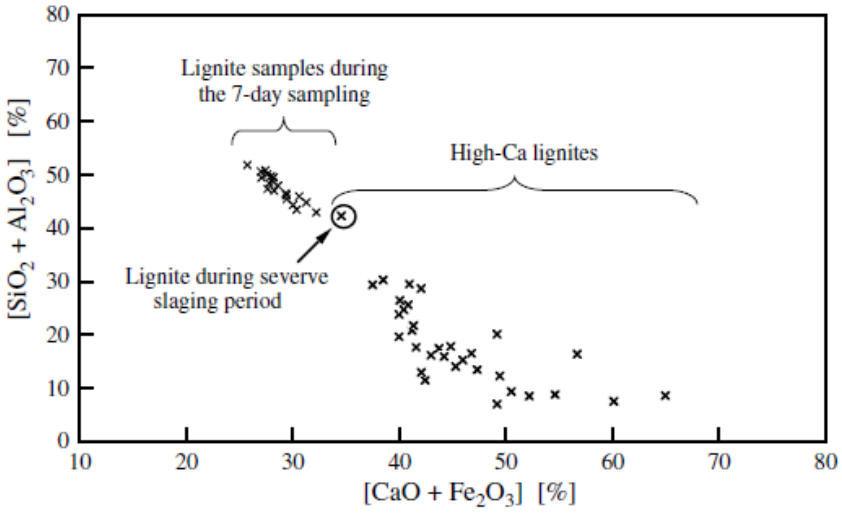

Figure 2.10 Correlation between major base oxides and acid oxides of lignite samples (Pipatmanomai et.al, 2009)

Luxsanayotin et al. (2010) reported the composition of minerals in the Mae Moh lignite as a function of the melting temperature of the ash. XRD analyses showed the presence of illite, pyrite and anhydrite in coal with 3.6% CaO. Anhydrite, known to lower ash melting temperature, was found to be the most abundant mineral in coal with 40.4% CaO. The coal that was expected to compete in the K1 and K3 were those with CaO 3.6 and 40.4 wt%, respectively. The AFT shows that their initial deformation temperatures were almost identical and low for the typical flue gas temperature in the radiation section. Similar IT was observed. The XRD analyses showed the presence of illite, pyrite and anhydrite in K1. Anhydrite, which is known to lower the IT, was also the most abundant mineral in K3. Phase diagram of the CaO-SiO_2-Al_2O_3 and Fe_2O_3 in the IT is shown in Figure 2.11. It is used as an indicator of the trends that affect the accumulation of ash melting the rough.

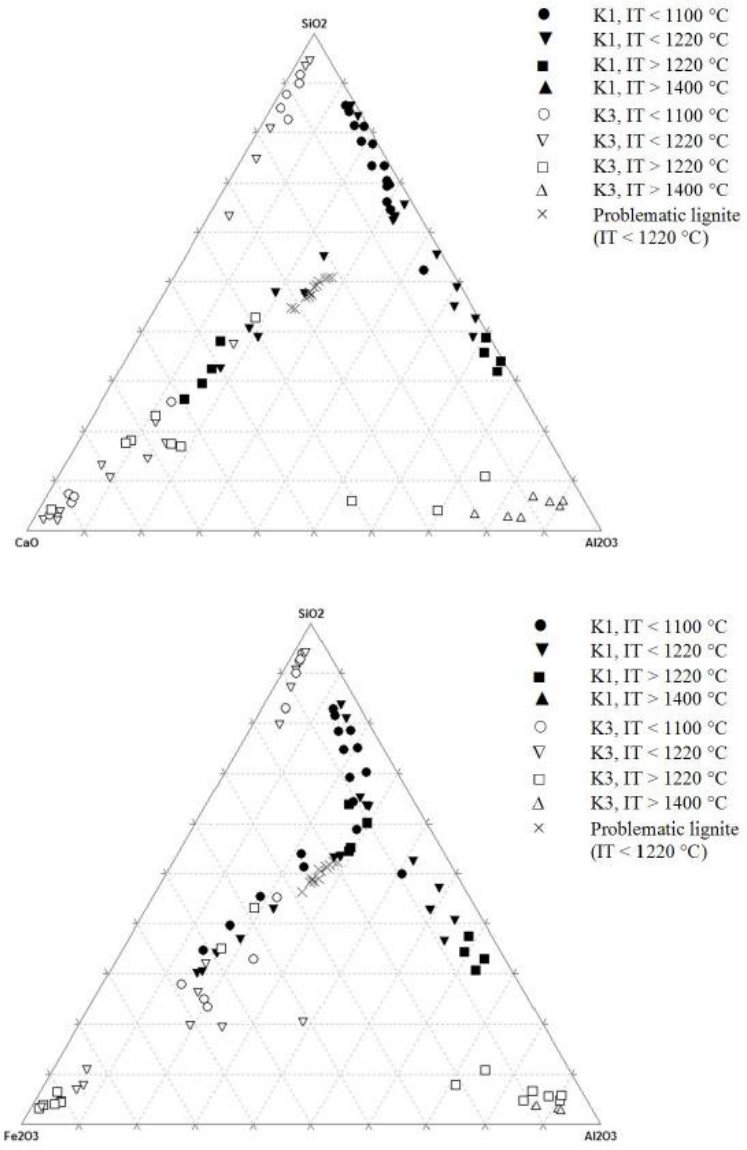

Figure 2.11 Ternary phase diagram of CaO-SiO_2-Al_2O_3 and Fe_2O_3 with the IT (Luxsanayotin et.al, 2010)

Song et al. (2009 a) showed the effect of CaO on fusion temperatures of ash in Figure 2.12. The temperatures decreased with increasing CaO content to 35%, after that the temperatures increased rapidly. Because of the sub-liquidus phase transforms from the anorthite phase to the gehlenite phase with increasing CaO content.

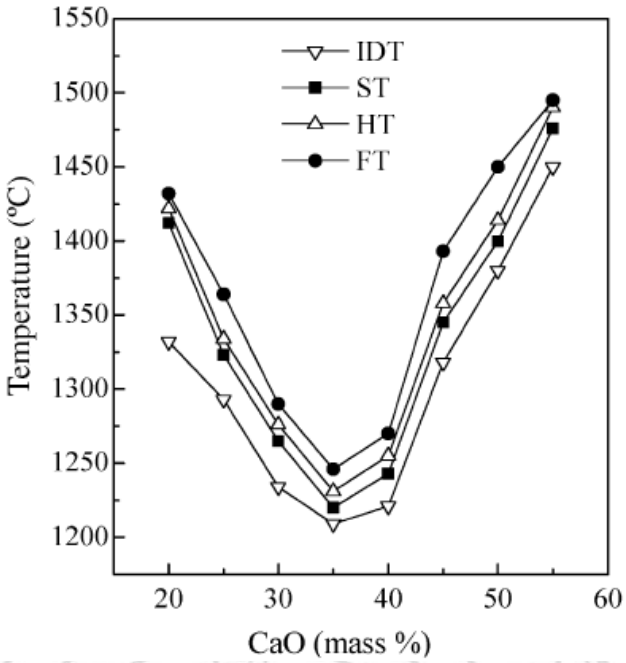

Figure 2.12 Ash fusion temperatures with different CaO content (Song et al., 2009 a)

Liu et al. (2013) studied the relationship between coal ash composition and ash fusion temperatures of seventeen coal samples, collected locally in China and abroad. The results in Figure 2.13 showed that the AFT temperatures decreased with the increasing Fe_2O_3. The CaO content was found to affect the AFT. Temperatures decreased reach a minimum value at 30% and then increased once again, which was different from Song et al. (2009 a).

From the previous research, factors that affect the boiler slag were identified. These approaches are useful in identifying problems occurred in Mae Moh. The suitable parameters with Mae Moh case were chosen to study in this work.

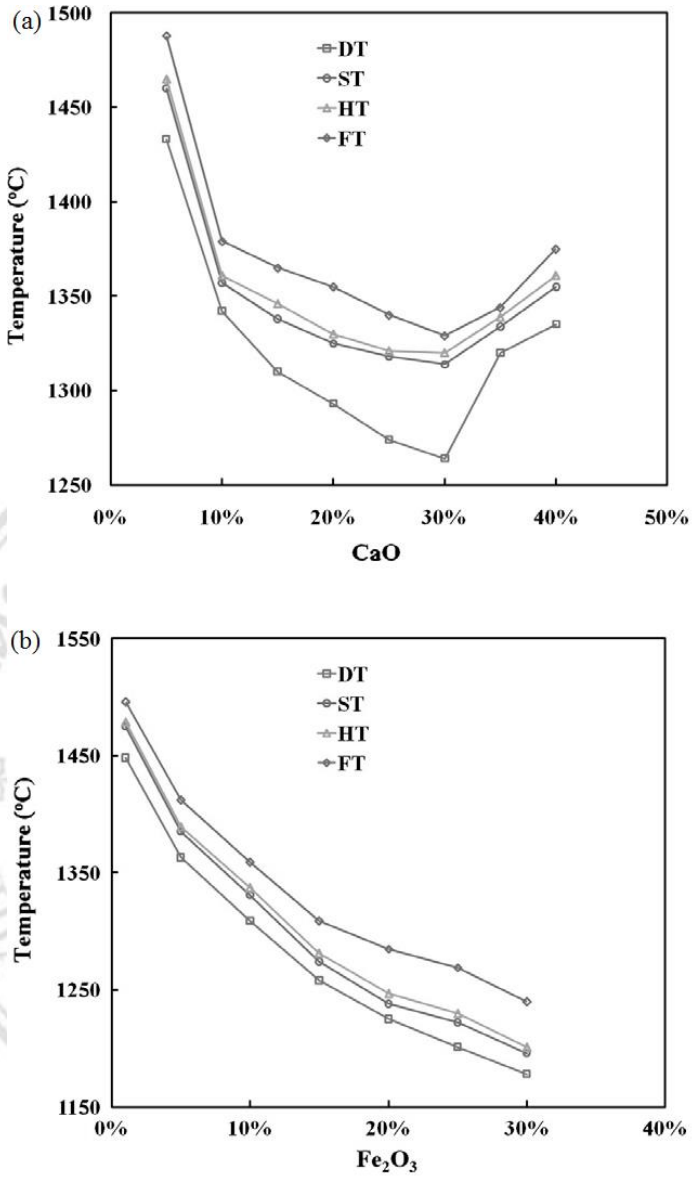

Figure 2.13 Ash fusion temperatures with different the percentage of oxides: (a) CaO content and (b) Fe_2O_3 content (Liu et al., 2013)

2.3.3 Prediction of Slag Occurrence

In this work, prediction slag was investigated separately using two methods. The first is the FactSage calculation and the second is the CFD simulation.

Consistent with the composition of the coal and ash, FactSage is commonly used to calculate the chemical reaction such as coal combustion, related to slag formation.

Jak (2002) used the F*A*C*T themodynamic package to predict multi-phase equilibria, liquidus temperatures and proportions of the liquid and solid phases. The results were applied to compare with coal ash fusion temperature from AFT test and slag characteristics from analysis which were mentioned previously.

Hanxu et al. (2006) used the FactSage thermodynamic model for predicting the Huainan coal ash behavior and AFT high temperature under reducing conditions of atmosphere. In addition, the ash transformation results from FactSage were consistent with the results from XRD.

Song et al. (2009 b) predicted the AFT temperatures of Chinese coal ash samples by FactSage program. The calculations were carried out in phase diagram with Ar and H_2 atmosphere at 1 atm pressure. The results shown in Figure 2.14, were in good agreement (standard error < 30°C) with AFT temperatures in both of Ar and H_2 conditions. The temperatures in H_2 atmosphere were always higher than the other because the iron oxides in ash were reduced to metallic iron, leading to mineral species and micromorphology changes.

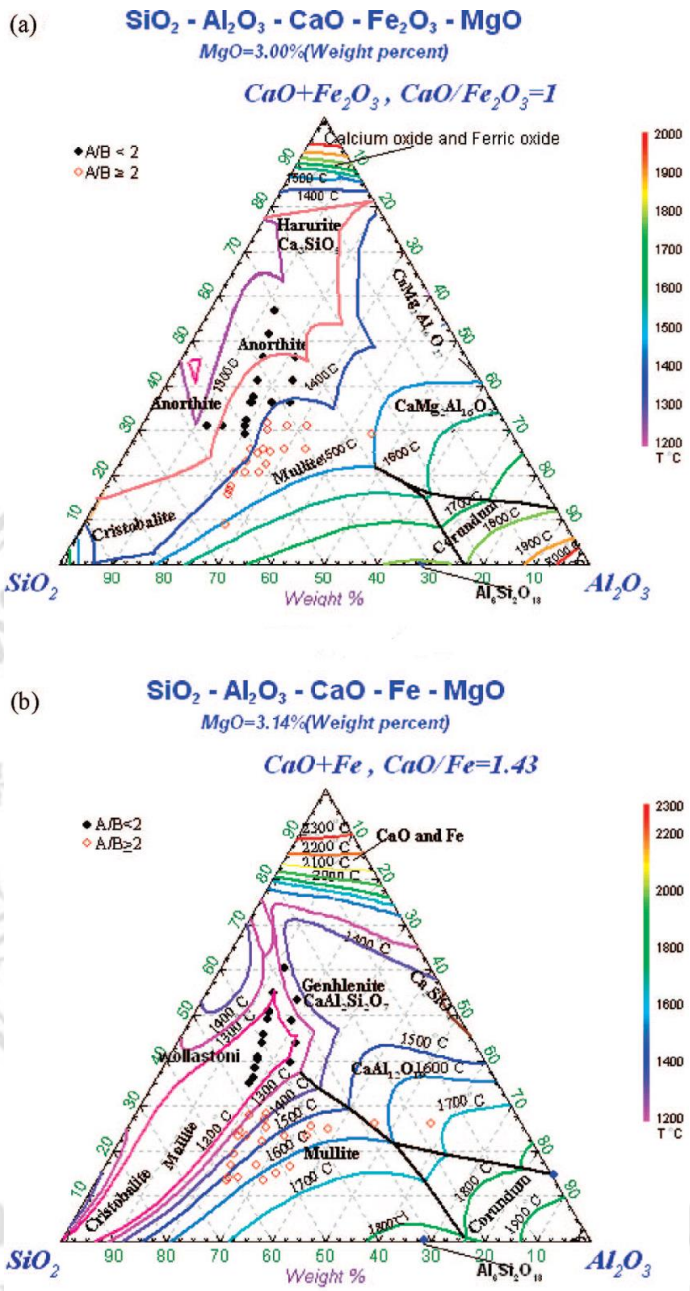

Figure 2.14 The equilibrium phase diagrams for the Si-Al-Ca-Fe-Mg-O system: (a) Ar atmosphere and (b) H_2 atmosphere

Song et al. (2010) used the FactSage software to calculate the liquidus temperatures and the proportions of the various phase of coal ash samples. The results were compared with measured AFT. The liquidus temperatures by phase equilibrium diagram showed parallel trends with higher than AFT (Song et al., 2009 b).

Van Dyk and Keyser (2012) studied the relationship between ash flow temperature and FactSage liquidus calculations temperatures. FactSage software with Equilib model was used to indicate the slag formation. The predicted results showed similar trend with AFT (accepted experimental error of AFT test range ±30°C). The CaO was significant contribution in total slag formation and mineral behavior, in the highlight conclusion of this research.

Garba (2012) predicted the melting behavior of slag from FactSage 6.2. The Equilib module was used to calculate the concentrations of chemical species from reaction to equilibrium. FToxid was used in database for slag. In Figure 2.15, the quantities of relevant species were shown at different temperatures of reaction. The composition of slag was detailed in Figure 2.16. One of the interesting conclusion in this work, the results from FactSage have been used to provide insight into some of the observations made during the CFD simulations.

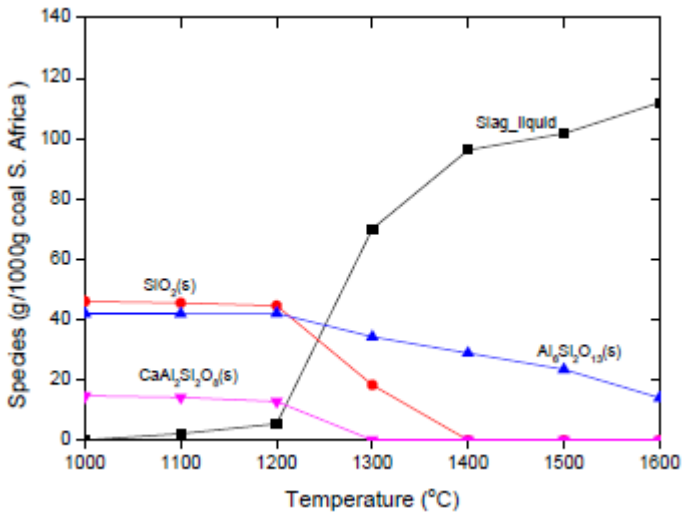

Figure 2.15 Mineral output from calculated the South African coal combustion (Garba, 2012)

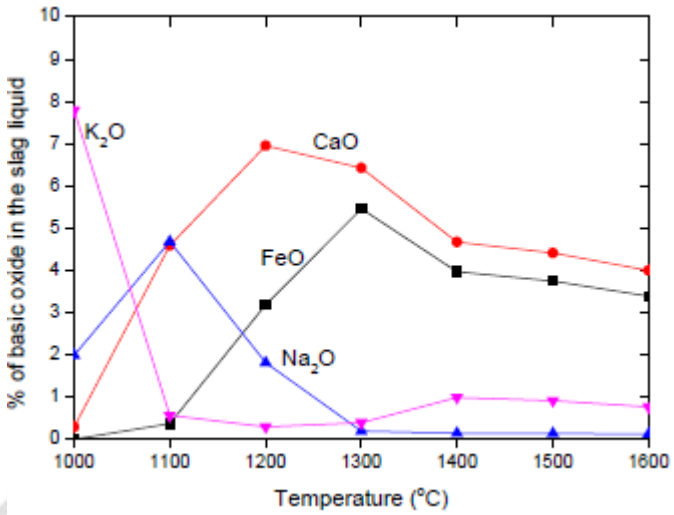

Figure 2.16 The percentage of oxide in slag from calculated the South African coal combustion (Garba, 2012)

Kong et al. (2013) explained the component of solid phase and change of liquid phase at different temperatures with CaO-SiO_2-Al_2O3-FeO system (Song et al., 2009) in FactSage program. The liquidus temperatures from phase equilibrium diagrams for pseudoternary systems correlated with AFT trends. It has been set up between FT temperature and liquidus temperature in Eq. 2.30.

$$T_{FT} = 86.86 + 0.86T_{liq} \quad (2.30)$$

FactSage (the fusion of two well-known software F*A*C*T/FACT-Win and ChemSage) is the largest thermochemical package and database available for inorganic solid and slag in the field of computational thermochemistry. The package runs on a PC operating under Microsoft Windows (Bale et al., 2002; Van Dyk et al., 2006; Bale et al., 2009). The Equilib module (thermodynamic application calculations) and Phase Diagram module (phase diagram calculations) were used to incorporate the FactSage Gibbs energy minimize (Eriksson and Konigsberger, 2008). These modules were

used to predict the ash behaviour, the ash fusion temperature, and quantify experimental results in this study.

In an attempt to simulate and predict the deposition of slag in boiler, the CFD has been used. For a better understanding, the reviews about deposition of slag in boiler are as follows.

Vasquez and Ma (2004) conducted the predictive methods and incorporate them into a CFD code. They used SmartBurn® for simulation model of Columbia tangentially fired boiler with 512 MW. The commercial tool resolves the Navier-Stokes equations and incorporates several numerical schemes for fluid flow, heat transfer, turbulence, and chemistry within the given geometry. The operating conditions can be set to simulate with the Discrete Phase Model (DPM), the Magnussen Hjertajer turbulence-chemistry interaction model, and Discrete Ordinate (DO) model. The output of the CFD model predicted the ash behavior, and provided a quantitative and quanlitative description of fireside slag formation within the furnace.

Ma et.al (2007) used AshPro^{SM} developed for a tangentially-fired furnace boiler of 512 MW power plant. Examples of the prediction of ash fusion furnace wall are shown in Figure 2.17. In Figure 2.18, the impact of the ash, on the thickness of the formation temperature, the hardness of the deposit on the walls of the furnace are shown. It was concluded that the impact of the ash was a major cause of the deposition, but may not correspond to the thickness of the deposit. It also depends on the furnace wall and the surface temperature of the ash to the hardness of the deposit, the temperature, chemical composition and thickness of the formation.

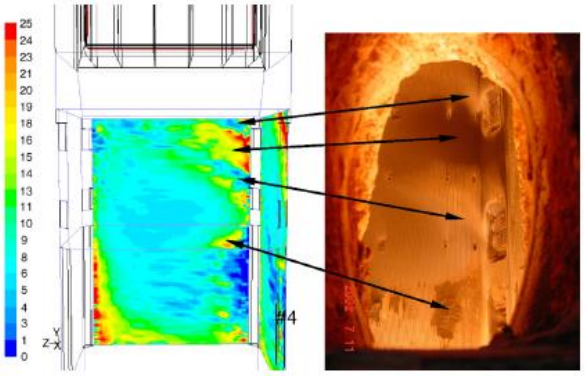

Figure 2.17 Deposit thickness (mm) on furnace wall and furnace wall picture at a similar location (Ma et.al, 2007)

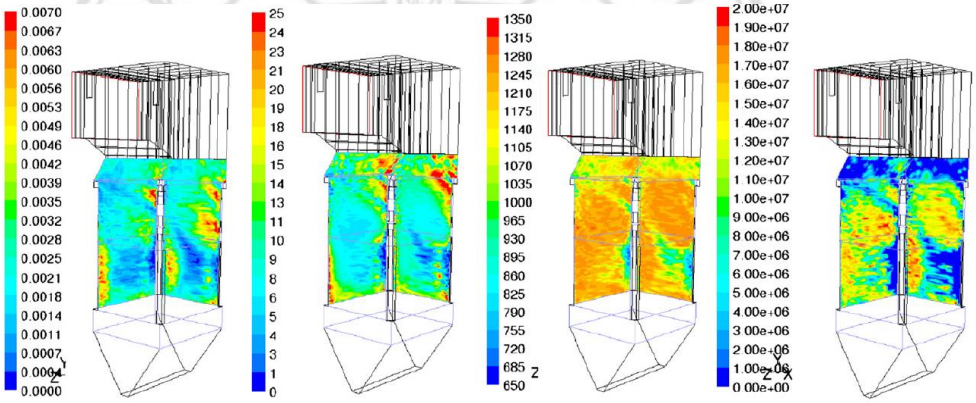

Figure 2.18 Ash impaction (kg/m2s), deposition thickness (mm), temperature (K), and deposition strength (Pa) on the furnace walls (Ma et.al, 2007)

Degereji et al. (2012) used CFD code to compute the temperature profiles and heat fluxes in the ACIRL furnace for four Australian coals. The calculation was based on one step reaction for combustion of the volatiles. The DO model was used in heat transfer between the particle and the boiler walls. The RNG k-ε model was used for turbulence. The discrete phase particle trajectory was employed. The results were compared with experimental data. The predicted flame temperatures were found to agree with measured and the predicted heat fluxes. The deposition model has been

developed for predicting the deposition rates of homogeneous coal ash slag in a high temperature zone. The results were not satisfactory.

Garba (2012) gave the steps of the deposition prediction by the FLUENT 12.1 software. First, the combustion furnace computational grid for using in the calculation was generated. Simulations were set up by selecting suitable models such as turbulence, heat transfer, chemical kinetics, etc., in an Eulerian frame of reference in order to establish the gas phase of the combustion processes. The parameters required to input into the software included the physical and chemical properties of the fuel and the operation conditions of the boiler. The coal with biomass co-combustion model was developed, but not mentioned in the report.

From the previous researches, CFD was used to solve fluid flow, turbulence, particle trajectory, heat transfer, chemical reactions of the fuel, and the wall heat flux. The methods will be used to predict the ash behavior and combined with the FactSage calculation for predicting slag behavior in this work.